

Wearable Electrodermal Activity Sensor for Real-Time Stress Detection Using Machine Learning

Salvador Santos^a, Joana Sousa^b and João Ferreira
NOS Inovação, Rua Actor António Silva, Lisbon, Portugal

Keywords: Wearable Technology, Electrodermal Activity (EDA), Stress Detection, Machine Learning, Real-Time Monitoring, Human-Computer Interaction, Biosensors, Arduino Nano ESP32.


Abstract: This paper discusses the design and implementation of a wearable electrodermal activity (EDA) sensor intended to detect subtle changes in skin conductivity, which are indicative of emotional states such as stress and anxiety, thus monitoring stress and arousal levels through advanced machine learning techniques. The device incorporates innovative conductive lycra combined with silver-silver chloride (Ag/AgCl) electrodes, enabling optimal skin contact and enhancing signal reliability. This integration allows for effective measurement of EDA. Utilizing the XGBoost algorithm, our machine learning model was trained on the ASCERTAIN dataset, achieving an overall accuracy of approximately 77% in predicting levels of arousal. While the model exhibited some challenges in predicting intermediate arousal states, it demonstrated strong precision and recall for extreme levels of arousal, underscoring its potential applications in mental health monitoring and human-computer interaction. The capabilities of this wearable technology for continuous and long-term health monitoring pave the way for further research into stress assessment and the understanding of emotional responses, emphasizing its relevance in enhancing psychological well-being.


1 INTRODUCTION

The autonomic nervous system (ANS) plays a pivotal role in regulating numerous physiological processes, including the production and distribution of sweat through eccrine sweat glands. This regulation is crucial for maintaining homeostasis and responding to various stimuli, including emotional states (Grimnes and Martinsen, 2015). The insulating properties of the skin and the conductive nature of sweat result in measurable differences in skin conductivity (Malmivuo and Plonsey, 1995). This is attributed to the activation of the ANS, which elevates sweat production in the sweat ducts during these emotional states. Despite the established link between emotional states and skin conductivity, there is a need for a wearable, reliable and non-invasive method to detect and quantify stress levels based on physiological responses. Current methods often lack the practicality or wearability required for continuous, real-time monitoring in everyday situations. A solution that addresses these limitations

could have profound implications for enhancing human-computer interactions, providing individuals with valuable insights into their emotional well-being (Bonato, 2003).

To study electrodermal activity (EDA), the signal is divided into skin conductance level (SCL) and skin conductance response (SCR), representing tonic and phasic components, respectively. The tonic activity (SCL) is a slowly changing base signal with frequencies below 0.02Hz. The phasic activity (SCR) arises from sympathetic activation and includes faster signals (frequencies <0.5Hz), characterized by significant fluctuations with amplitudes of 0.05 μ S or higher, occurring within 3 seconds after a stimulus. Phasic activation can be event-related (ER-SCR) following a stimulus or spontaneous (NS-SCR) due to normal sympathetic regulation. As represented in figure 1, an SCR signal typically appears as a small bump on the SCL, with distinct rise and decay phases (Boucsein, 2012).

^a  <https://orcid.org/0009-0003-4523-5567>

^b  <https://orcid.org/0000-0002-6418-2312>

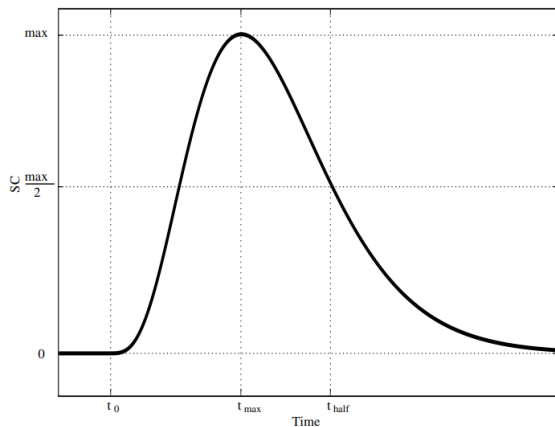


Figure 1: Graphic representation of an SCR event.

The primary objective of this research is to develop a wearable sensor capable of detecting subtle changes in skin conductivity associated with arousal and anxiety. By analyzing these EDA (electrodermal activity) signals using machine learning algorithms, the sensor will generate a stress score. Beyond mere detection, the project aims to translate physiological information into customized actions or feedback for the user.

What sets this project apart as innovative is its pioneering integration of a wearable device with advanced machine learning technology specifically designed to detect arousal in real-time. This capability allows the sensor to analyze electrodermal activity (EDA) signals as they occur, providing immediate feedback to users based on their physiological responses. Such a dynamic interaction creates a highly personalized experience, empowering users to gain insights into their emotional states and manage stress or anxiety more effectively.

The implications of this research extend well beyond mere stress detection. By leveraging real-time machine learning analysis of physiological data, the project aims to cultivate the development of more empathetic and responsive technologies. This could greatly enhance various applications, such as optimizing user experience in digital interfaces or providing timely therapeutic interventions for individuals grappling with stress or anxiety. Ultimately, the project aspires to make significant contributions to the field of human-computer interaction by weaving emotional well-being into the fabric of technological design.

2 RECORDING SITE SELECTION

Electrodermal activity (EDA) is crucial in psychophysiological research, typically measured on the palms due to their high density of eccrine sweat glands - 600-700 glands/cm² (Boucsein, 2012). However, for practical, non-invasive wearable technology, the wrist is an excellent alternative.

Eccrine sweat glands are distributed throughout the body, with the forearm, including the wrist, having about 108 glands/cm². A study by van Dooren et al. (2012) found that the wrist demonstrated intermediate skin conductance responsiveness and ranked high for S-AMPL (sum of skin conductance responses per minute), comparable to traditionally preferred sites like the fingers and feet. The wrist also showed significant correlation ($r = .55$ to $.59$) with finger measurements, suggesting it can reliably reflect traditional EDA data.

The wrist offers practical advantages: it is accessible, comfortable for prolonged wear, integrates seamlessly with existing wearable devices like smartwatches, and is less intrusive than high-density sites like the palms.

While palms are the gold standard for EDA measurement, the wrist is a practical and reliable alternative for wearables. Its responsiveness, correlation with traditional sites, and user-friendly advantages make it ideal for non-invasive EDA recording, supporting applications in psychophysiological research and personal health monitoring.

3 MEASURING DEVICE

3.1 Selection and Implementation of a Circuit

Based on the literature review and the state of the art, it was decided that the circuit that seemed most appropriate to measure electrodermal activity, taking into account the objective of incorporating it into a wearable device, was the one described by Poh et al. (2010) from M.I.T. It offers a small size, a reduced number of components, an EDA measuring range within the required values and has no need for the calibration of its amplification in contrast with other circuits that work with a variable gain, facilitating its usability and the complexity of post-measuring processing of the obtained EDA signals.

Given the exploratory nature of this project, its feasibility had to be ensured with limited and easily obtained resources. Thus, the decision was made to start the construction of this circuit using the most widely used A/D converter available in the market: an Arduino Board. While there are several types of Arduino Boards, the necessity of maintaining a small scale for the measuring circuit and the incorporation of it into a wireless wearable device – to ensure usability – made it clear that the Arduino Nano ESP32 was the optimal choice. It has the smallest size among its counterparts and benefits from the ESP32-S3 microcontroller, which provides full Arduino support for wireless and Bluetooth® connectivity. Additionally, literature indicates that an EDA signal requires at least 12-bit resolution for reliable measurement (Boucein, 2012), and the Arduino Board meets this requirement. Consequently, the circuit would be powered by the 3.3V pin, the dual amplifier by the 5V pin, with both components grounded via the GND pins from the Arduino Board. Furthermore, both measuring wires would connect to the analog pins to record the voltage received in each case.

Moreover, initial components were chosen, with price being a major factor since the device is still in prototype phase. For the resistors, coal resistors of 0.25W with a tolerance of 5% were picked. For the 0.1µC capacitors, the decision was to use ceramic capacitors. Finally, to act as the two amplifiers, the dual precision operational amplifier LT1013 was selected. In the case of the dual operational amplifier, although the LM358 was the cheapest option, the importance of reducing the oscillation of the amplifier to better obtain the EDA signal made it a non-viable choice, thus the choice of the dual amplifier of higher cost, but also better performance.

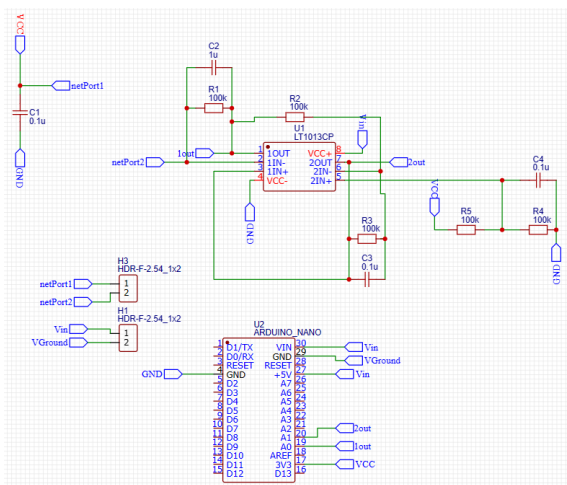


Figure 2: Final circuit configuration.

A scheme of the final circuit configuration can be observed in figure 2.

3.2 Simulation, Analysis, and Experimental Validation of Circuit Performance

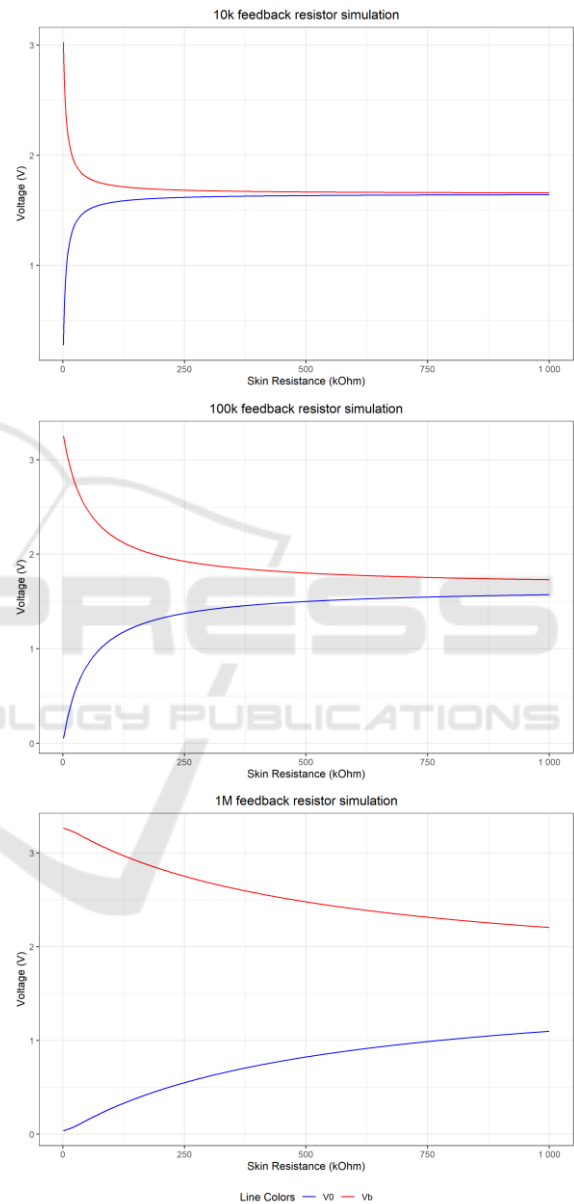


Figure 3: Graphic representations of simulations conducted in LTSpice for feedback resistor of 10kΩ, 100kΩ, and 1MΩ, respectively from top to bottom.

While the preliminary selection of the circuit and its components had been established, a comprehensive analysis of the analog circuit remained pending to

Table 1: Experimental results of prototype with 10k Ω feedback resistance.

Resistance (k Ω)	972	461	216	99.0	46.0	21.0	9.83	4.60
Conductance (μ S)	1.03	2.17	4.63	10.1	21.7	46.5	101	217
Measured mean value (μ S)	1.019	2.173	4.549	9.994	21.49	45.63	101.9	218.7
Standard Deviation (%)	9.76	3.66	2.38	0.82	0.60	0.16	0.29	0.05
Accuracy (%)	0.95	0.19	1.74	1.06	1.13	1.90	0.11	0.58

Table 2: Experimental results of prototype with 100k Ω Feedback Resistance.

Resistance (k Ω)	972	461	216	99.0	45.5	21.5	9.83	4.60
Conductance (μ S)	1.03	2.17	4.63	10.1	21.7	46.5	102	217
Measured mean value (μ S)	1.037	2.184	4.644	10.16	21.97	47.54	109.5	254.2
Standard Deviation (%)	1.17	0.72	0.35	0.27	0.31	0.36	0.44	1.27
Accuracy (%)	0.75	0.68	0.32	0.56	0.03	0.17	7.59	16.95

Table 3: Experimental results of prototype with 1M Ω Feedback Resistance.

Resistance (k Ω)	968	461	217	98.0	46.0	21.0	9.84	4.61
Conductance (μ S)	1.03	2.17	4.61	10.2	21.7	48.8	101	217
Measured mean value (μ S)	1.031	2.172	4.684	10.65	24.77	65.08	319.5	991.3
Standard Deviation (%)	0.18	0.25	0.31	0.66	1.30	1.7	10.7	8.97
Accuracy (%)	0.21	0.15	1.63	4.40	14.0	33.4	214	357

validate the previously assumed potentials and limitations of the circuit. Consequently, a simulation of the circuit was executed utilizing the LTspice free software. Given the skin's function as a potentiometer, with its conductance continually varying due to both internal and external influences, a DC operating point analysis (op.) was conducted by systematically varying the resistance values associated with the skin. In this DC operating point simulation, incremental steps were taken for the parameter X, representing the skin resistance, ranging from 1k Ω to 1M Ω — the spectrum of potential values for skin contact resistance, as indicated by existing literature — using intervals of 1k Ω . The measured conductance values were observed to be predominantly influenced by the feedback resistance of the amplifier directly connected to the skin. Consequently, simulations were conducted with varying orders of magnitude for this resistance (10k Ω , 100k Ω , and 1M Ω) to assess their impact on the measurements.

Figure 3 depicts simulations conducted in LTspice and graphically represented using the R programming language. The upper and lower lines in each graph correspond to the voltage levels of the 1out and 2out measuring pins connected to the Arduino board in the final circuit representation, as

shown in Figure 2. Notably, an observable trend emerges wherein an increase in feedback resistance results in a more linear trajectory for both measured voltages. This effect becomes particularly pronounced at the termination point of the plot, corresponding to a skin resistance of 1M Ω . The anticipated behaviour, derived from a previously formulated expression, posits hyperbolic curves as an accurate representation of the measured voltages.

Furthermore, the inclination of the curves holds significance in determining measurement sensitivity. A more inclined slope suggests heightened sensitivity. While one might intuitively select a 1M Ω feedback resistor for the initial amplifier due to its nearly linear behaviour within the requisite skin resistance range, the simulation results reveal deviations at lower resistances. Specifically, when employing a 1M Ω feedback resistor, the voltages cease to conform to hyperbolic curves at skin resistances below approximately 60k Ω , indicating amplifier saturation.

Consequently, the simulation outcomes advocate for the adoption of a 100k Ω feedback resistor in the proposed circuit for optimal performance across the entire spectrum of skin resistance values. This configuration demonstrates superior sensitivity, while avoiding deviation at lower resistances, making

it the most suitable choice for the intended measurements.

The culmination of the circuit analysis, encompassing the three specified values of feedback resistance ($10\text{k}\Omega$, $100\text{k}\Omega$, and $1\text{M}\Omega$), entailed the construction of prototypes to evaluate the accuracy and precision of each distinct circuit. For a comprehensive assessment of these parameters across the entire range of skin resistance, measurements were executed using seven different resistors ($4.7\text{k}\Omega$, $10\text{k}\Omega$, $22\text{k}\Omega$, $47\text{k}\Omega$, $100\text{k}\Omega$, $220\text{k}\Omega$, and $470\text{k}\Omega$, and $1\text{M}\Omega$) for each of the three circuits. In each instance, 1000 samples were collected over a 5-minute interval. The reference values assigned to each resistor were determined with a multimeter, considering and compensating for their 5% tolerance. The ensuing results are tabulated in this paper. Each table lists resistance values measured with the multimeter alongside their corresponding conductance measurements, the means of conductance values measured by the prototypes, and their standard deviations and accuracy percentages. In the provided tables, accuracy was quantified as the percentage deviation between the reference conductance value of the resistors and the mean conductance value obtained through measurement.

Consistent with the simulations, the circuit featuring $1\text{M}\Omega$ feedback resistors exhibits noteworthy deviations at resistances below approximately $60\text{k}\Omega$, corresponding to conductance values exceeding $16\mu\text{S}$. Given that normal skin conductance can extend up to $30\mu\text{S}$, this particular circuit proves unsuitable for the intended measurements.

Upon comparing the circuits with $10\text{k}\Omega$ and $100\text{k}\Omega$ feedback resistors, it becomes evident that the latter demonstrates superior accuracy performance up to conductance values of approximately $50\mu\text{S}$, in line with the specified range of skin conductance values. Furthermore, it exhibits acceptable performance in terms of standard deviation, with a maximum deviation of 1.17%.

Consequently, based on the insights derived from both simulations and experimental tests on the three distinct circuits, it has been conclusively demonstrated that the circuit featuring a $100\text{k}\Omega$ feedback resistor is the most suitable for the intended measurements. Finally, to adapt to the alteration in feedback resistance, it is imperative to adjust the value of the capacitor connected in parallel to $1\mu\text{F}$ to ensure the preservation of the low-pass filter effect with a cut-off frequency of 1.6Hz .

3.3 PCB Design and Fabrication

Utilizing the standard EasyEDA editor, the circuit schematics were drafted, and employing one of the editor's tools, these schematics were subsequently transformed into a PCB design, depicted in figure 4. Following this, a BOOM and Gerber file were imported, facilitating the subsequent stages of PCB fabrication and assembly. The manufacturing process of the PCB board was carried out by the Chinese PCB manufacturer JCLPCB. The ensuing assembly procedures were executed by the manufacturer, with the exception of the Arduino Nano board. The latter was soldered to the PCB board personally by our team.

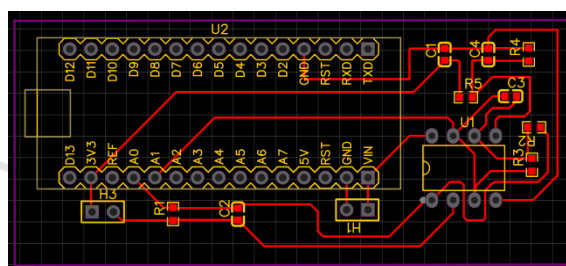


Figure 4: Configuration of the final circuit PCB.

3.4 Electrode Selection, Implementation and Optimization

Silver-silver chloride electrodes have consistently proven to be the most suitable for recording skin conductance (Geddes et al., 1969), and they have been consistently recommended by experts (Fowles et al., 1981; Boucsein et al., 2012). However, dry usage without electrolytes applied is generally not advised. This is because applying the electrode metal directly to the skin can lead to gradual humidity accumulation under the metal plate, resulting in instability and a drift towards increased conductance over time (Fowles et al., 1981). Hence, dry silver/silver chloride (Ag/AgCl) electrodes may progressively become less comfortable and dependable, potentially leading to irritation of the skin at the contact area.

In order to address these issues, given that long-term electrodermal activity (EDA) measurement is still in its early stages of development, there has been a necessity to explore alternative electrode materials. These materials should be capable of better conforming to the skin's irregular shape and facilitating seamless contact between the skin and the electrode. Several studies (Poh et al., 2010; Banganho, 2019) have investigated various options, including

conductive fabrics, conductive leathers, and 3D-printed electrodes crafted from polylactic acid (PLA). These materials have undergone rigorous testing and comparison with the traditional Ag/AgCl dry disc electrodes, which are considered the gold standard.

Since the referred publication of António Bangalho's MSc thesis (2019), the developer of MedTex P130, Shieldex[®], has introduced new conductive lycras that enhance their previous offerings. One such advancement is Shieldex[®] Technik-tex P130+B, a knitted fabric metallized with silver tailored specifically for the medical and smart wearables industries. This material represents a hybrid knitted fabric comprising 78% polyamide and 22% elastane. The elastane is intricately knitted in both the warp and weft directions, rendering this highly conductive textile stretchable on both axes and well-suited for flexible applications in smart textiles. Building upon its predecessors, Technik-tex P130+B improves upon its electrical surface resistance, decreasing from $4.2\Omega/\text{square}$ to $<2\Omega/\text{square}$. Furthermore, the applied coating (+ B) safeguards the silver against mechanical stress, a common occurrence in wearables, aligning with the primary purpose of the devised device. With this information in mind, integrating this advanced conductive lycra with Ag/AgCl dry electrodes proves to be a significant asset for the EDA measurement circuit. Therefore, it is the selected electrode implementation for the intended apparatus.

Regarding electrodes contact area, as the contact area diminishes, the potential for error due to electrode paste seepage increases, leading to lower conductance levels and reduced response amplitudes. Consequently, it's advisable to avoid small contact areas. A recommended area of 1.0 cm^2 (corresponding to approximately 11 mm in diameter) is suggested where the recording site allows. If achieving an area of this size is not feasible, then the maximum area permitted by the recording site should be utilized (Fowles et al., 1981). Because of market availability challenges, dry Ag/AgCl disc electrodes with a diameter limit of 10 mm were ordered for the specified device. This slight deviation from the original plan shouldn't be of significant concern due to its reduced size.

4 COMMUNICATION PROTOCOL

With all device parameters set, there is the need to establish the communication protocol for acquiring

conductance measurements from the device. This protocol involves three key parties: the measuring device, a remote server, and a local machine.

The first party, the measuring device, has already been described in this report. It will communicate with all other parties via WiFi. The next component is the remote server, which operates through a specific link, stores data in BigQuery, and runs a machine learning model — all using Google Cloud Platform services. Finally, the local machine features a user-friendly interface that allows users to send commands to the measuring device and receive measured data and model predictions from the remote server. This local machine can be a personal computer or a smartphone with an app installed, though the app design and implementation will be left as part of future iterations of this project, as for now, it remains a proof of concept.

In conclusion, the communication protocol effectively integrates the measuring device, remote server, and local machine, ensuring seamless data acquisition and processing. This setup lays the foundation for future enhancements and iterations, particularly in developing a comprehensive application for broader use.

5 MACHINE LEARNING MODEL: TRAINING AND TESTING

5.1 Dataset Selection

The final step of this project involved training and testing a machine learning (ML) model for future integration into the EDA measuring device. According to the project objectives, the ML model needs to be trained to use statistical features from the EDA signal as input and provide predictions on the user's stress/arousal levels based on a previously trained stress score. To train the ML model, a dataset containing EDA signals along with corresponding arousal scores — either self-reported or assessed by external observers — was required. Among the proposed datasets, the ASCERTAIN dataset (Subramanian et al., 2018) was deemed the most suitable and easily accessible.

The ASCERTAIN dataset includes big-five personality scales and emotional self-ratings from 58 users, along with synchronously recorded EDA data and other physiological signals collected using off-the-shelf sensors while the users watched affective movie clips. This dataset met all the criteria for an

acceptable training and testing dataset due to its diverse subjects and comprehensive affective movie clips paired with self-reported arousal scores.

Before using the dataset, the EDA signals had to be pre-processed for usability and analysis. Each time the signal is analysed, it will be passed through a 2Hz low-pass filter to eliminate high-frequency noise, as recommended and tested in previous work by Gamboa and Fred (2007).

5.2 Statistical Features Selection

Selecting the appropriate statistical features from the EDA signals was a crucial step before training and testing. The statistical features for this project were based on those used in prior research by Jennifer Healey and Rosalind Picard (2005). The initial features included the mean and variance of the normalized signal, the total number of SCRs (skin conductance responses) in the analysed segment, the sum of the magnitudes of these responses, the sum of response durations, and the sum of the estimated areas under these responses. The algorithm for detecting these responses was based on the one proposed in the PhD thesis of H. Gamboa (2008).

Finally, a statistical analysis of the features obtained from the dataset was performed to refine model performance. This analysis involved shuffling the data and removing outliers, followed by an analysis of variance (ANOVA) and a correlation study between features.

The ANOVA results were positive, with all features displaying very low p-values and very high F-statistics, indicating their statistical significance. However, the correlation study revealed a very weak correlation – absolute correlations values always below 0.4 – for the mean and variance of the normalized signals with all other features. Consequently, these two features were dropped from the subsequent training and testing phases. This left the model with the remaining four statistical features.

5.3 Model Selection

The XGBoost model was selected for training and testing due to its widely acknowledged capabilities in classification tasks. It is renowned in the literature for its exceptional performance (Sagi and Rokach, 2021; Chen and Fai, 2021), particularly in handling sparse data that often contain missing values or zeros. Moreover, XGBoost scales seamlessly from small to large datasets, maintaining high accuracy even with extensive data volumes.

Additionally, XGBoost integrates regularization techniques to prevent overfitting, ensuring it captures meaningful patterns rather than merely memorizing the training data. It adeptly manages imbalanced datasets and offers interpretability features that provide insights into model decisions. Furthermore, XGBoost effectively handles multicollinear data, thereby ensuring robust predictions in scenarios with correlated predictors.

Overall, XGBoost is celebrated for its versatility, interpretability, and robustness, making it a preferred choice for both academic research and practical applications in classification tasks.

5.4 Model Performance

At last, training and testing of the selected model was performed. The results from our model, including performance metrics and cross-validation outcomes, provide valuable insights into its effectiveness and reliability in this task.

The model's classification report offers a comprehensive evaluation of its predictive performance across seven arousal categories (ranging from 0 to 6). Precision, recall, and F1-score metrics vary across these categories, reflecting the model's ability to distinguish between different arousal states. Notably, the model achieves high precision and recall – above the 90% and for most close to 99% – for low arousal levels (0 and 1) and the maximum arousal level (6), indicating robust performance in identifying extreme arousal states. However, in intermediate arousal levels, precision and recall metrics show a gradual decline – values fluctuate between the 50th and the 80th percentile. This suggests that the model faces challenges in accurately predicting medium arousal states based on the statistical features from EDA signals.

The overall accuracy score on the test set is approximately 77%, indicating an acceptable performance in predicting arousal levels across the dataset. Cross-validation results further validate this performance, with an average accuracy score of approximately 77% across different folds. This consistency suggests that the model generalizes well to unseen data, a crucial aspect for its practical application.

In conclusion, while our model shows promising results in predicting arousal levels from EDA signals using statistical features, there remains room for improvement, particularly in enhancing the prediction accuracy for intermediate arousal states. Future research could explore additional features to address these challenges effectively. Nonetheless, the

demonstrated reliability in cross-validation underscores the potential of our approach for automated arousal level assessment, with implications for fields such as mental health monitoring and human-computer interaction.

6 FUTURE WORKS AND IMPROVEMENTS

This research has laid the groundwork for the integration of electrodermal activity (EDA) measuring devices with machine learning models for arousal level prediction. However, several avenues for future work can be explored to enhance the results and expand the application of our findings.

First, while the XGBoost model achieved an overall accuracy of approximately 77%, there is room for improvement, particularly in accurately predicting intermediate arousal states. Future studies could focus on experimenting with alternative machine learning algorithms, such as deep learning models or ensemble methods, to improve prediction accuracy across all arousal levels.

Second, expanding the feature set used for training the machine learning model may lead to better classification performance. Investigating additional physiological signals, such as heart rate variability (HRV) or environmental variables, could provide a more comprehensive understanding of stress and arousal levels.

Conducting longitudinal studies to assess the effectiveness of the wearable device in real-life situations is essential. Future research can involve testing the device across various contexts — such as workplaces, social gatherings, or during relaxation exercises — to provide insights into its usability and effectiveness in actual settings.

Additionally, creating an engaging and intuitive user interface for the application would enhance user experience. Incorporating features like real-time feedback, personalized stress management recommendations, and tracking capabilities could significantly increase user engagement and utility.

Exploring novel electrode materials or configurations could further enhance comfort and accuracy in skin conductance measurements. Comparative studies of different materials will help optimize the design for diverse user needs.

Moreover, incorporating our device with other products presents an exciting opportunity to gain valuable insights into users' arousal states, which can significantly enhance their interactive experiences

with those products. By integrating the wearable sensor with applications in gaming, virtual reality (VR) environments, or even automotive systems, we can adapt these experiences in real time based on the users' emotional and physiological responses. For instance, gaming applications could adjust difficulty levels or narrative elements depending on the player's stress or excitement levels, creating a more immersive and tailored experience. Similarly, in VR settings, the content could dynamically shift to either calm or engage users based on their arousal state, promoting emotional well-being. In the context of driving, our device could trigger alerts or adjustments to vehicle settings to enhance safety or comfort based on detected stress levels. This adaptability not only enriches user experience but also fosters improved human-computer interaction by ensuring that technology aligns more closely with the emotional needs of its users.

Finally, in the course of our experiments measuring skin conductance using different configurations of the circuit from Poh et al. (2010) on the wrists of some team members, we observed an intriguing phenomenon. The typical EDA signal, consisting of its tonic and phasic components, appeared to be modulated by a distinct periodic signal. Upon analysing this modulation, we concluded that it is likely associated with the heart rate of our team members.

This discovery opens up a promising direction for future iterations of our device. By utilizing this modified configuration of the original circuit, we could develop a wearable device capable of simultaneously measuring both electrodermal activity (EDA) and heart rate variability (HRV) signals. Incorporating HRV measurements alongside EDA could significantly enhance the accuracy of stress detection, as both physiological metrics provide complementary insights into the body's stress response. This two-in-one measurement capability could lead to more nuanced and effective stress management applications, ultimately offering users a better understanding of their emotional and physiological states.

By pursuing these avenues, future research can further enhance the utility of EDA measurements in mental health monitoring and provide innovative solutions for stress management and emotional well-being.

7 CONCLUSION

This paper successfully demonstrated the integration of an electrodermal activity (EDA) measuring device with a robust communication protocol and a machine learning model for stress and arousal level prediction. By selecting the most suitable materials and configurations for the device, including the use of a 100k Ω feedback resistor and silver-silver chloride electrodes, we ensured accurate and reliable conductance measurements.

The communication protocol effectively linked the measuring device, a remote server, and a local machine, facilitating seamless data acquisition and processing. This setup serves as a foundation for future developments, particularly in creating a comprehensive application for broader usage.

The machine learning model, trained using the ASCERTAIN dataset and implemented with the XGBoost algorithm, achieved an overall accuracy of approximately 77% in predicting arousal levels. Despite challenges in accurately predicting intermediate arousal states, the model's acceptable precision and recall for extreme arousal levels underscore its potential for practical applications in mental health monitoring and human-computer interaction.

Overall, the project lays a solid groundwork for future enhancements and iterations, with significant implications for the automated assessment of arousal levels and related applications. Future research should focus on improving model performance for intermediate arousal states and exploring additional features to enhance prediction accuracy. Additionally, future research should also focus on implementing this device in a useful application where it enhances human-computer interaction or daily stress monitoring. This will not only validate the practical utility of the device but also pave the way for its integration into everyday technologies aimed at improving emotional well-being and user experience.

REFERENCES

- Boucsein, W., Fowles, D. C., Grimnes, S., Ben-Shakhar, G., Roth, W. T., Dawson, M. E., Filion, D. L., & Society for Psychophysiological Research Ad Hoc Committee on Electrodermal Measures (2012). Publication recommendations for electrodermal measurements. *Psychophysiology*, 49(8), 1017–1034. <https://doi.org/10.1111/j.1469-8986.2012.01384.x>.
- Banganho, A. F. R. (2019). *Electrodermal activity sensor (EDA) with adaptive gain control* (Master's thesis, Instituto Superior Técnico).
- Bonato, P. (2003). Wearable sensors/systems and their impact on biomedical engineering. *IEEE Engineering in Medicine and Biology Magazine*, 22(3), 18–20. <https://doi.org/10.1109/memb.2003.1213622>
- Chen, Z., & Fan, W. (2021). A freeway travel time prediction method based on an XGBOOST model. *Sustainability*, 13(15), 8577. <https://doi.org/10.3390/su13158577>
- Fowles, D. C., Christie, M. J., Edelberg, R., Grings, W. W., Lykken, D. T., & Venables, P. H. (1981). Publication recommendations for electrodermal measurements. *Psychophysiology*, 18(3), 232–239. <https://doi.org/10.1111/j.1469-8986.1981.tb03024.x>
- Gamboa, H.F., Fred, A.L., & Telecomunicações, I.D. (2007). An Electrodermal Activity Psychophysiological Model Gamboa, H. F. S. (2008). *Multi-modal behavioral biometrics based on HCI and electrophysiology*. (Doctoral dissertation, Universidade Técnica de Lisboa).
- Geddes, L. A., Baker, L. E., & Moore, A. G. (1969). Optimum electrolytic chloriding of silver electrodes. *Medical & Biological Engineering*, 7(1), 49–56. <https://doi.org/10.1007/bf02474669>
- Grimnes, S., & Martinsen, Ø. G. (2015). Bioimpedance and bioelectricity basics. In *Elsevier eBooks*. <https://doi.org/10.1016/c2012-0-06951-7>
- Healey, J., & Picard, R. (2005). Detecting stress during Real-World driving tasks using physiological sensors. *IEEE Transactions on Intelligent Transportation Systems*, 6(2), 156–166. <https://doi.org/10.1109/tits.2005.848368>
- Malmivuo, J. (1995). The electrodermal response. In *Oxford University Press eBooks* (pp. 428–434). <https://doi.org/10.1093/acprof:oso/9780195058239.003.0027>
- Van Dooren, M., De Vries, J., & Janssen, J. H. (2012). Emotional sweating across the body: Comparing 16 different skin conductance measurement locations. *Physiology & Behavior*, 106(2), 298–304. <https://doi.org/10.1016/j.physbeh.2012.01.020>
- Poh, N. M., Swenson, N. C., & Picard, R. W. (2010). A wearable sensor for unobtrusive, Long-Term assessment of electrodermal activity. *IEEE Transactions on Biomedical Engineering*, 57(5), 1243–1252. <https://doi.org/10.1109/tbme.2009.2038487>
- Subramanian, R., Wache, J., Abadi, M. K., Vieriu, R. L., Winkler, S., & Sebe, N. (2016). ASCERTAIN: Emotion and personality recognition using commercial sensors. *IEEE Transactions on Affective Computing*, 9(2), 147–160. <https://doi.org/10.1109/taffc.2016.2625250>
- Sagi, O., & Rokach, L. (2021). Approximating XGBoost with an interpretable decision tree. *Information Sciences*, 572, 522–542. <https://doi.org/10.1016/j.ins.2021.05.055>